Mol Neurobiol (2014) 49:199–215
DOI 10.1007/s12035-013-8511-x

tPA Regulates Neurite Outgrowth by Phosphorylation of LRP5/6 in Neural Progenitor Cells

Sung Hoon Lee · Hyun Myung Ko · Kyoung Ja Kwon · Jongmin Lee · Seol-Heui Han · Dong Wook Han · Jae Hoon Cheong · Jong Hoon Ryu · Chan Young Shin

Received: 18 April 2013 / Accepted: 8 July 2013 / Published online: 8 August 2013

Abstract Despite the important role of tissue plasminogen activator (tPA) as a neuromodulator in neurons, microglia, and astrocytes, its role in neural progenitor cell (NPC) development is not clear yet. We identified that tPA is highly expressed in NPCs compared with neurons. Inhibition of tPA activity or expression using tPA stop, PAI-1, or tPA siRNA inhibited neurite outgrowth from NPCs, while overexpression or addition of exogenous tPA increased neurite outgrowth. The expression of Wnt and β-catenin as well as phosphorylation of LRP5 and LRP6, which has been implicated in Wnt–β-catenin signaling, was rapidly increased after tPA treatment and was decreased by tPA siRNA transfection. Knockdown of β-catenin or LRP5/6 expression by siRNA prevented tPA-induced neurite extension. NPCs obtained from tPA KO mice showed impaired neurite outgrowth compared with WT NPCs. In ischemic rat brains, axon density was higher in the brains transplanted with WT NPCs than in those with tPA KO NPCs, suggesting increased axonal sprouting by NPC-derived tPA. tPA-mediated regulation of neuronal maturation in NPCs may play an important role during development and in regenerative conditions.

Keywords Neural progenitor cell · Tissue plasminogen activator · Neurite outgrowth · LRP5/6 · β-Catenin

Sung Hoon Lee and Hyun Myung Ko contributed equally to this work.

S. H. Lee · H. M. Ko · K. J. Kwon · J. Lee · S.-H. Han · C. Y. Shin
Department of Neuroscience, School of Medicine and Center for Neuroscience Research, IBST, Konkuk University, Hwayang-dong, Gwangjin-gu, Seoul 143-701, Republic of Korea

D. W. Han
Department of Stem Cell Biology, School of Medicine, Konkuk University, 1 Hwayang-dong, Gwangjin-gu, Seoul 143-701, Republic of Korea

D. W. Han · C. Y. Shin
Institute of Functional Genomics, Konkuk University, 1 Hwayang-dong, Gwangjin-gu, Seoul 143-701, Republic of Korea

J. H. Cheong
College of Pharmacy and Uimyung Research Institute for Neuroscience, Sahmyook University, Seoul, Republic of Korea

J. H. Ryu (✉)
Department of Life and Nanopharmaceutical Sciences, Kyung Hee University, 1 Hoeki-dong, Dongdaemoon-Gu, Seoul 130-701, Republic of Korea
e-mail: jhryu63@khu.ac.kr

C. Y. Shin (✉)
Department of Pharmacology, School of Medicine, Konkuk University, 1 Hwayang-Dong, Gwangjin-Gu, Seoul, Republic of Korea
e-mail: chanyshin@kku.ac.kr

Introduction

Tissue plasminogen activator (tPA) is a serine proteinase, which is one of the most widely expressed and extensively studied proteinases in the central nervous system [1–3]. tPA is involved in a variety of physiological and pathological processes, including neurite outgrowth, synaptic plasticity, and neuronal survival. Regulation of neurite outgrowth by tPA is involved in plasminogen activation [4] and plays an important role in pathological or regenerative conditions. Recently, axon remodeling induced by transplantation of bone marrow stromal cell (BMSC) in the stroke damaged brain was suggested to be modulated by the induced protein expression and activity of tPA in astrocytes [5]. In addition, tPA was reported to be localized in regenerating axons and the activity of tPA was increased over 7 days in a sciatic nerve crush model [6]. Interestingly, a tPA−/− animal showed delayed behavioral recovery after sciatic nerve injury which suggests the essential role of tPA in the modulation of axonal regeneration [7]. Despite the relatively extensive array of data suggesting the role of tPA in neurite outgrowth, the mechanism is still unclear.

The Wnt pathway is one of the essential regulators of neurite outgrowth. Wnt increased β-catenin expression by inhibiting the activity of GSK3β, leading to activation of downstream target gene transcription [8] and regulation of neuronal axon guidance and synapse remodeling [9, 10]. Endogenous β-catenin lies on presynaptic sites, and localization of β-catenin in growth cones plays a crucial role in the regulation of axon remodeling [11]. Interestingly, tPA may regulate the concentration level of β-catenin and phosphorylation of GSK3β in several cell types, including ECV 304 carcinoma cells and rat kidney interstitial fibroblasts [12, 13].

Regarding the regulation of the Wnt pathway, two distinct cell surface receptors, Frizzled and low-density lipoprotein receptor-related protein 5/6 (LRP5/6) have been assigned an essential role of transmitting signals from Wnt to β-catenin. While Frizzled, a seven-transmembrane protein, has a crucial role in both Wnt–β-catenin and noncanonical Wnt signaling pathways, a single-pass membrane protein LRP5/6 has a specific role in the direct regulation of the Wnt–β-catenin pathway [14–19]. When Wnt binds to Frizzled and LRP5/6, a series of molecular interaction leads to the formation of LRP5/6 signalosome which stabilizes β-catenin by modulating phosphorylation of the intracellular domain of LRP5/6 or direct regulation of GSK3β [20, 21]. LRP is a member of the low-density lipoprotein receptor family interacting with several ligands, including tPA, uPA, and ApoE [22]. LRP is also implicated in the regulation of neurite outgrowth [23, 24]. Considering the essential role of LRP5/6 in the regulation of the Wnt pathway, it would be interesting to hypothesize that LRP5/6, upstream of GSK3β and β-catenin, binds to tPA and regulates neurite outgrowth induced by tPA.

The expression of tPA was reported in all cell types of the CNS, including astrocytes, neurons, microglia, and oligodendrocytes [25–30]. Moreover, the role of tPA in the developing brain has been suggested [31, 32]. The expression of tPA in neural progenitor cells (NPCs) and its possible role in neural development, however, have not been reported yet. Here, we report that tPA is expressed in rat NPCs and modulates neurite outgrowth by regulating the Wnt–GSK3β–β-catenin pathway, at least in part, through phosphorylation of LRP5/6.

Materials and Methods

Primary Neural Progenitor Cell Culture

All experimental procedures were performed by means of protocols approved by the Institutional Animal Care and Use Committee of the Konkuk University. NPC culture was prepared from the embryonic cortex of an E14 Sprague–Dawley (SD) rat [33] (DBL, Chungbuk, Republic of Korea) or E12 mouse [34] as reported previously with slight modifications. In brief, cortices were dissociated into single cells by pipetting several times and were passed through a 40-μm strainer (BD Bioscience, Franklin Lakes, NJ, USA). Single cells were incubated with Dulbecco's modified Eagle's medium (DMEM)/F12 (Invitrogen, Carlsbad, CA, USA) supplemented with B27 (Invitrogen), 20 ng/ml EGF (Millipore, Billerica, MA, USA), and 10 ng/ml bFGF (Invitrogen) in a 5 % CO_2, 90 % N_2, and 5 % O_2 incubator. These single cells grew into a floating neurosphere and then were dissociated into single cells again with trypsin–EDTA (Invitrogen) and regrew into a neurosphere in B27-, EGF-, and FGF-containing media. This procedure was repeated once again and neurosphere colonies were dissociated again into single cells for further experiments. To induce differentiation of NPCs, cells were plated onto a poly-L-ornithine (Sigma, Saint Louis, MO, USA)-coated plate with DMEM/F12 media containing 2 % penicillin/streptomycin without the addition of any growth factors or serum. The cells were differentiated at 37 °C in a humidified atmosphere with 5 % CO_2, 90 % N_2, and 5 % O_2.

Primary Neuron Culture

Primary neuron culture was prepared from E18 embryo of SD rats (DBL) according to a previously published procedure [35]. In brief, cortices were dissociated into single cells by pipetting several times with a Pasteur pipette. Cells were plated onto a poly-D-lysine (Sigma)-coated plate or glass cover slips with Neuro-basal medium (Invitrogen) supplemented with 2 % penicillin/streptomycin, 2 mM glutamine (Invitrogen), and B27 (Invitrogen), in a 5 % CO_2, 90 % N_2, and 5 % O_2 incubator. Neurons were incubated for 8 days with half replacement of the media every third day.

Determination of Neurite Outgrowth

NPCs were plated at low densities (20,000 cells/cm^2) to avoid cellular contact. An immunofluorescence image of Tuj-1 staining was captured using an upright fluorescence microscope BX61 (Olympus) 3 or 10 days after treatment. The neurite was analyzed using the image analysis software, MetaMorph (Molecular Devices, CA, USA). The neurite was defined as the processes protruding from the cells longer than the length of the cell soma, which did not contact other neurites or cell bodies. To verify the accuracy of neurite outgrowth analysis, captured images were analyzed again with ImageJ (National Institutes of Health, Bethesda, MD, USA). For each treatment group, actual measurements of neurite length and branch number were performed by two observers in a double-blind manner.

tPA Zymography

Zymography was performed for semiquantitative analysis of tPA activity secreted into the culture medium as described previously [36, 37] with slight modifications. In brief, culture supernatants were mixed with 4X zymo sample buffer (8 %*w*/*v* SDS, 40 % glycerol, 200 mM Tris–HCl, pH 6.8, and 0.02 % bromphenol blue) in the absence of reducing agents. Samples were separated by electrophoresis using 8 % SDS-polyacrylamide. Thereafter, the gel was washed twice in 2.5 % Triton X-100 for 30 min and then incubated for 14 h at 37 °C in a reaction buffer (20 mM Tris–HCl, 166 mM $CaCl_2$, pH 7.6). After staining the gel with PowerStain™ Brilliant Blue R250 (Mbiotech, Kyunggi-do, Republic of Korea), it was destained using destaining solution (10 % acetone, 20 % MeOH, 70 % DDW). The molecular weight of plasmin-dependent caseinolytic activity was estimated by markers of known molecular weight (Fermentas, Harrington Court, Burlington, Canada). The gel was pictured with a LAS-3000 Imaging Densitometer (Fuji, Quansys Biosciences, UT, USA). In some cases, the optical density of the area of each clear band was determined using ImageJ.

Western Blot

Western blot was performed according to a previously published procedure [38]. A total amount of 20–40 μg of proteins was collected from the cells with RIPA buffer (150 mM NaCl, 50 mM Tris, pH 8.0, 0.5 % sodium deoxycholate, 0.1 % SDS, 1 % Triton X-100). Separation of protein bands was performed using 8 % SDS-polyacrylamide gel electrophoresis, and proteins were electrically transferred onto nitrocellulose transfer membranes (Whatman, Hahnestraβe, Dassel, Germany). The membranes were blocked with 5 % dried skim milk at 4 °C overnight. Membranes were then incubated overnight with an antibody directed against Nestin (1:5,000; Millipore), Tuj-1 (1:10,000; Covance, Princeton, NJ, USA), GFAP (1:5,000; Dako, Carpinteria, CA, USA), synaptophysin (1:10,000, BD Bioscience, Franklin Lakes, NJ, USA), GAD (1:5,000; Millipore), PSD-95 (1:5,000; Chemicon, Millipore), tPA (1:2,000; Santa Cruz, CA, USA), LRP5 (1:2,000; Abcam, Cambridge, MA, USA), LRP6 (1:2,000; Abcam), GSK3β (1:5,000; Cell Signaling), pGSK3β (1:5,000; Cell Signaling, Danvers, MA, USA), β-catenin (1:5,000; Santa Cruz), pLRP5 (1:2,500; Abnova, Walnut, CA, USA), pLRP6 (1:2,500; Abnova), Wnt5a (1:5,000; Abcam), Wnt7a (1:2000; Santa Cruz), Wnt7b (1:2,000; Abcam), and β-actin (1:20,000; Sigma). The membranes were washed three times with TBS–Tween (0.2 % Tween-20) for 5 min each, followed by incubation with horseradish peroxidase-conjugated secondary antibody for 90 min at room temperature. The membranes were developed with enhanced chemiluminescence solution (Amersham, Buckinghamshire, UK) according to the manufacturer's instructions. The developed protein bands were detected with LAS-3000 (Fujifilm, Minato-ku, Tokyo, Japan). The signal intensity of blots was analyzed using ImageJ software. To analyze the level of Wnt in the extracellular matrix fraction, cells were detached from plates using 1 mM EDTA in PBS and then rinsed twice. The remaining extracellular matrix (ECM) proteins on the plates were collected by scraping with 2× SDS loading buffer and boiled for 5 min at 90 °C prior to analysis by Western blot.

Immunofluorescence Staining

Differentiated NPCs on the cover glass were fixed with 4 % paraformaldehyde (PFA) at 37 °C for 20 min. The fixed cells were treated with 0.1 % Triton X-100 for 15 min at room temperature and washed with PBS. The cells were incubated overnight at 4 °C with primary antibodies. After washing three times with PBS, secondary antibodies conjugated with either Alexa Fluor® 594 Dye (1:500; Invitrogen) or Alexa Fluor® 488 Dye (1:500; Invitrogen) were diluted in blocking buffer and incubated for 1 h at room temperature. After washing three times, the cover glass was mounted in Vectashield (Vector, Burlingame, CA, USA) and visualized with a Zeiss LSM 700 Confocal (Carl Zeiss).

Reverse Transcriptase-Polymerase Chain Reaction (RT-PCR)

Total RNA was extracted using Trizol reagent (Invitrogen). Reverse transcription was conducted for 40 min at 45 °C with 2 μg of total RNA using 1 U/μl of superscript II reverse transcriptase (GibcoBRL). Oligo (dT) was used as a primer for this reaction. The extracted RNAs were heated at 94 °C for 5 min to terminate the reaction. The cDNA obtained from 2 μg of total RNA was used as a template for PCR amplification of tPA, Wnt7a, and glyceraldehyde 3-phosphate dehydrogenase (GAPDH) mRNA. The primer sequence was as follows: tPA, forward: TCAGATGAGATGACAGGGAAATGCC, reverse: ATCATACAGTTCTCCCAGCC, 385 bp; Wnt7a, forward: GGAGAAGCAAGGCCAGTACC, reverse: TTGTCCTTGAGCACGTAGCC, 288 bp; and GAPDH, forward: TCCCTCAAGATTGTCAGCAA, reverse: AGATCCACAACGGATACATT, 555 bp. PCR amplification was performed in 25~35 cycles (94 °C, 1 min; 55 °C, 1 min; 72 °C, 1 min). After the last cycle step, all PCR samples were incubated for an additional 10 min at 72 °C. The final products were analyzed with 1.0 % agarose gel electrophoresis and stained with ethidium bromide. The gel was photographed under ultraviolet light.

Immunoprecipitation

Immunoprecipitation was performed as described previously with minor modifications [39]. Briefly, NPCs were lysed with ice-cold lysis buffer (50 mM HEPES, pH 7.5, 150 mM NaCl, 1 mM EDTA with proteinase inhibitor) and centrifuged at 16,100×*g* for 20 min at 4 °C. A total of 700 μg of NPC lysates was incubated overnight with 2 μg of tPA antibody at 4 °C. Normal rabbit or goat IgGs of the same concentration were used as negative controls. Protein A agarose (Thermo Scientific, Waltham, MA, USA) was added to the mixture and incubated overnight at 4 °C. The samples were washed three times and eluted with 2× SDS sample buffer for Western blot analysis.

Crosslinking

Crosslinking of proteins interacting with tPA was conducted as described previously [40]. NPCs were incubated with HEPES buffer (120 mM NaCl, 5.4 mM KCl, 0.8 mM $MgCl_2$, 20 mM HEPES, 15 mM glucose, 1.8 mM $CaCl_2$, pH 7.4) solution at 4 °C for 1 h. Crosslinking was performed with 10 μmol/l 3,3′-dithiobis(sulfosuccinimidylpropionate) (DTSSP) (Thermo Scientific) at 4 °C for 2 h, and the reaction was stopped by washing two times with 20 mmol/l Tris buffer, pH 7.5. The cells were lysed and analyzed by immunoprecipitation using tPA antibody as described above.

Transfection

NPCs were transfected with plasmid expressing GFP, tPA-GFP (kindly donated by Dr. Bethe Scallatter), or siRNA constructs against tPA, β-catenin, and LRP 5/6 using Lipofectamine 2000 (Invitrogen). Rat tPA-specific siRNA Stealth RNAi™ siRNA Select RNAi was purchased from Invitrogen (cat. no. RSS304050). LRP5- and LRP6-specific siRNA siGENOMESMARTpool Rat LOC312781 and LOC293649 were purchased from Dharmacon. β-Catenin siRNA was purchased from Invitrogen (cat. no. RSS331356). As negative controls, NPCs were transfected with control siRNAs containing the same content of GC as target siRNAs. NPCs were plated at a density of 200,000 cells/cm^2 on a plate. Transfection conditions such as transfection time and concentration of DNA/RNA were adjusted according to the manufacturer's guide for Lipofectamine™ 2000. The cells were harvested with RIPA buffer 24 h or 3 days after transfection or fixed with 4 % PFA for further experiment.

Middle Cerebral Artery Occlusion (MCAO)

All procedures were approved by the Institutional Animal Care and Use Committee of the Konkuk University. Briefly, 8-week-old male SD rats (Orient Co., Ltd, a branch of Charles River Laboratories, Seoul, Republic of Korea) weighing 280 to 300 g were used for MCAO surgery. The animals were anesthetized with xylazine/zoletil (1:2, 30 mg:60 mg/kg, i.p.). A 4–0 nylon suture was then introduced into the ICA via an incision on the ECA stump and advanced through the carotid canal until it became lodged in the narrowing of the anterior cerebral artery, blocking the origin of the middle cerebral artery to stop the flow of blood. The blood flow was monitored using a laser Doppler system (Doppler PeriFlux System 5000, PERIMED, Stockholm, Sweden). Reperfusion was performed by removal of the filament 1 h after endovascular suturing. The animals were maintained at 37±1 °C during surgery using a heating pad equipped with a temperature controller (CMA140, POLYGEN, Poland). After awakening from anesthesia, they were allowed to have food and water ad libitum and were used for NPC transplantation experiments.

Transplantation of Mice NPCs into Ischemic Rat Brain

NPCs were isolated from WT and tPA KO mice and transplantation of NPCs was performed according to the methods described previously [41]. Rats (n=6) were first anesthetized with xylazine/zoletil (1:2) for 24 h after MCAO surgery. NPC cell density was adjusted to ~25,000 viable cells per microliter and a 4-μl solution was injected at 1 μl/min into the striatum (AP=+2, L=−5, V=+0.7) of each rat using the stereotaxic injection system (Stoelting Co., IL, USA). Before removal of the needle, 2 min of waiting time was allowed for cells to settle down. The solution containing cells was injected with a 25-μl Hamilton syringe (Hamilton Company USA, Energy Way, Reno, NV, USA). As negative controls, control rats were injected only with the same volume of culture medium. The transplanted animals were recovered and maintained in standard 12 h dark/light cycle with free access to food and water. After 2 weeks, the rats were sacrificed for axon and myelin analysis.

Bielshowsky and Luxol Fast Blue Staining

The fiber of the axon–myelin bundle in the striatum was stained using Bielshowsky and Luxol fast blue staining as reported previously [42]. Briefly, frozen slides of 5 μm in thickness were placed in 20 % silver nitrate in the dark, then in ammoniacal silver solution. The slides were developed until brown and washed with ammonia water. The slides were then placed overnight in Luxol fast blue staining solution at 60 °C. After washing with 95 % alcohol, the slides were placed in lithium carbonate solution and 70 % alcohol solution repeatedly. After rinsing with water, the slides were stained with cresyl violet. The stained slides were observed under an optical microscope and analyzed using a Micro Computer Imaging Device (MCID) analysis system

(Imaging Research, St. Catharines, Ontario, Canada) to detect the density and length of axons, which appear dark over a blue background. Randomly selected nine fields were analyzed per animal.

Statistical Analysis

Data are expressed as mean ± standard error of mean (SEM). Statistical significance was analyzed by Student's *t* test or one-way analysis of variance (ANOVA) followed by Turkey's post hoc comparison. A p value<0.05 was considered significant.

Results

We first examined the expression of tPA in NPCs. Cultured NPCs or neurons were plated to have the same density (120,000 cells/cm^2), and the culture media were analyzed for tPA protein expression and enzymatic activity (Fig. 1a) by Western blot and casein zymography, respectively. The identity of both cell types was verified using cell-type-specific markers such as Nestin (for NPCs) and PSD-95, Tuj-1, and synaptophysin (for neurons). The level of tPA protein in NPCs was higher compared with neurons (Fig. 1a; 399.41±21.78 % vs neuron); the tPA zymographic activity was also increased (Fig. 1a; 180.96±2.14 % vs neuron). We also confirmed the expression of tPA mRNA in NPCs by RT-PCR. Furthermore, sequence analysis showed an authenticity of rat tPA mRNA in cultured NPCs (gene no.: NM_013151.2, data not shown). We also checked the expression and the activity level of plasminogen activator inhibitor-1 (PAI-1, an endogenous inhibitor of tPA) protein; however, we could not detect a significant level of expression of PAI-1 in rat NPCs (data not shown).

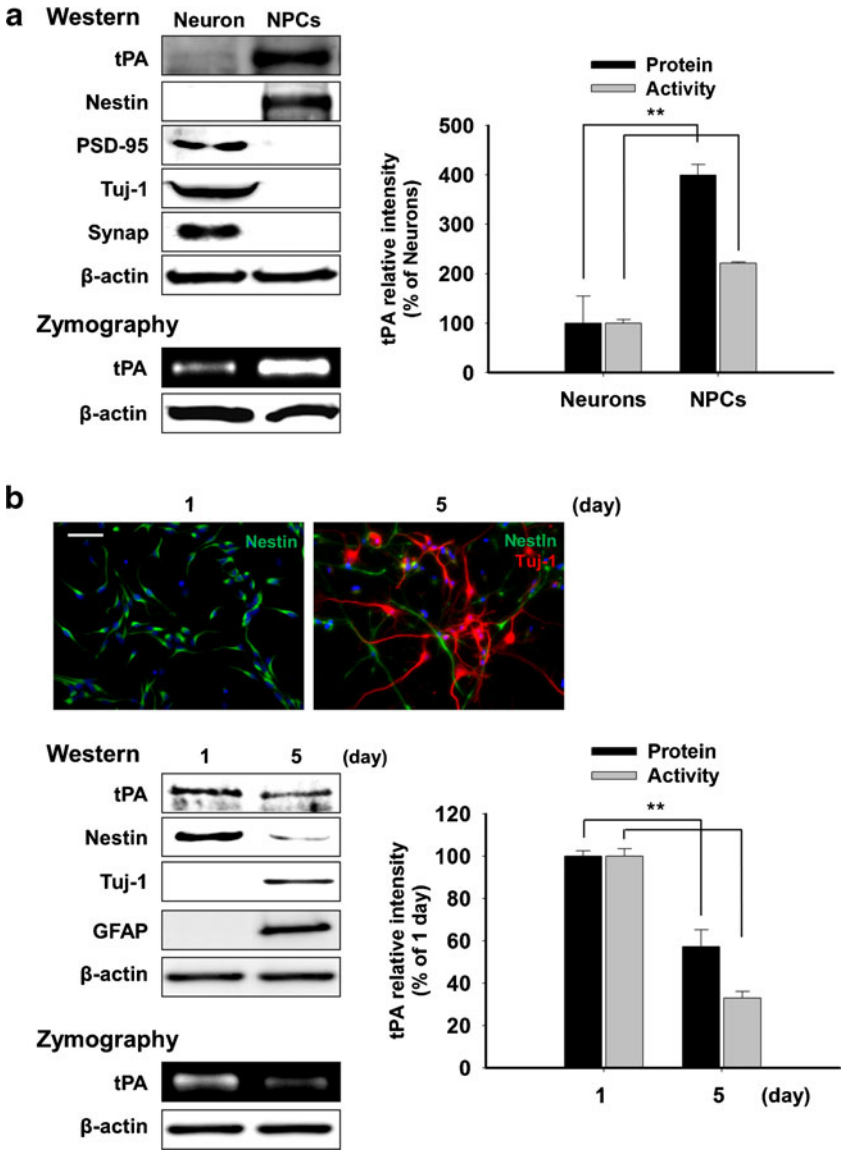

Fig. 1 Protein expression and activity of tPA in NPCs. **a** Higher activity and expression level of tPA protein in NPCs compared to neurons. Western blot was performed with antibodies against tPA and cell-specific markers. PAI-1 was not detected in both types of cells. Activity of tPA in NPCs and neurons was determined by zymography, as described. **b** The effect of NPC differentiation on protein expression and activity of tPA. NPCs were differentiated for 1 or 5 days in vitro. Immunocytochemistry data showed that NPCs (*left panel*, *green*) were differentiated into neurons (*right panel*, *red*) at day 5. Scale bar=50 μm. Western blot showed that the expression levels of Nestin and tPA were decreased, while those of Tuj-1 and GFAP were increased with differentiation of NPCs. For the determination of tPA activity by zymography, medium was changed into fresh medium 24 h before collection. Values represent mean ± SEM. $^{**}p<0.01$, statistically significant difference (Student's *t* test, $n=3$)

To verify higher protein expression and enzymatic activity of tPA in NPCs compared with neurons, we checked protein expression and enzymatic activity of tPA after differentiation of NPCs into neurons. NPCs were differentiated into neurons for 5 days by removing growth factors. As expected, the level of tPA was decreased in differentiated cells as expected (Fig. 1b), suggesting that the tPA expression level was decreased along the progression of differentiation of NPCs into neurons.

To determine the role of tPA on NPC differentiation, NPCs were plated at a density of 20,000 cells/cm^2 and were incubated with exogenous tPA for 3 days without growth factors to induce differentiation. Neurite extension was analyzed by immunocytochemistry against Tuj-1. As shown in Fig. 2a, neurite outgrowth was increased by tPA. For vehicle-treated NPCs and 1 μg/ml of tPA-treated NPCs, the branch numbers were 3.25±0.29 and 5.75±0.53, and the neurite lengths were 91.79±6.91 and 186.33±19.88 μm, respectively. In Western blot analysis, the expression of Nestin—an NPC marker—was decreased by tPA and the expression of Tuj-1 was increased in the tPA-treated group after 10 days from the induction of differentiation compared with vehicle-treated controls (Fig. 2b). The expressions of both inhibitory neuronal marker GAD and excitatory neuronal marker PSD-95 were increased by tPA, and most notably, the expression of presynaptic marker protein synaptophysin was greatly increased by tPA (Fig. 2b). This suggests that tPA is primarily involved in the increase of axonal outgrowth and neuronal maturation rather than cell type specification. The expression of glial cell marker GFAP was not significantly changed by tPA.

To unequivocally demonstrate the importance of endogenous tPA on neurite outgrowth from NPCs, we used a chemical and an endogenous inhibitor of tPA, namely, tPA stop and PAI-1. NPCs were incubated with tPA stop and PAI-1 for 3 days under the differentiation condition. Although most cells still expressed Nestin with very little expression of Tuj-1 on the first day of differentiation, the length and number of cellular processes outgrowing from Nestin-positive NPCs were decreased by both tPA stop and PAI-1 (Fig. 2c). Induction of differentiation reduced the expression of Nestin, and tPA stop and PAI-1 prevented the normal decrease in Nestin expression, which resulted in a higher number of Nestin-positive cells compared with vehicle-treated controls (Fig. 2c). On differentiation day 3, neurite outgrowth from NPCs was inhibited by tPA stop or PAI-1 (Fig. 2c). Likewise, in Western blot analysis, the expression of Nestin was higher in the tPA stop-treated group on day 1 (Fig. 2d) and the expression of Tuj-1 as well as other neuronal markers such as GAD, PSD-95, and synaptophysin was decreased by tPA stop without any effects on GFAP expression 10 days after induction of differentiation (Fig. 2d).

Fig. 2 tPA increased neurite outgrowth in NPCs. **a** NPCs were incubated with tPA (0.5, 1 μg/ml) for 3 days and the cells were immunostained using antibodies for Tuj-1 (*red*) and Nestin (*green*). Statistical significance was analyzed by one-way ANOVA (**$p<0.01$, *$p<0.05$). In **c**, NPCs were incubated with tPA stop (1 μM) or PAI-1 (40 ng/ml) for 3 days. On each cover glass, nine fields were randomly selected and over 50 neurons were chosen for analysis of neurite length and branch number. Values represent mean ± SEM (Student's *t* test, **$p<0.01$, *$p<0.05$, $n=3$). Scale bar=100 μm. **b** NPCs were differentiated for 1 or 10 days with tPA or **d** tPA stop (1 μM), and the differentiated cells were harvested for Western blot analysis against cell type-specific marker proteins. $n=5$. Statistical significance was analyzed by one-way ANOVA (**$p<0.01$, *$p<0.05$). **e** Time-lapse phase contrast image series showing neurite outgrowth in NPCs. NPCs were plated at low density and images were captured until 72 h after treatment, as described. Branch number and neurite length were analyzed as described in "Materials and Methods." Scale bar=50 μm. $n=4$. **f** NPCs were transfected with GFP and tPA-GFP and differentiated for 3 days. In each sample, more than 20 transfected cells were analyzed for neurite outgrowth. Scale bar=50 μm. $n=3$. **g** NPCs were transfected with tPA siRNA, and RT-PCR, Western blot, and tPA zymography were performed to confirm the expression of tPA. **h** siRNA-transfected NPCs were differentiated for 3 days and immunostained with Tuj-1. At least 20 cells were analyzed from three independent experiments. Scale bar=100 μm. **i** siRNA-transfected NPCs were differentiated for 10 days and harvested for Western blot analysis using astroglial and neuronal markers

To analyze the kinetics of neurite outgrowth in situ, we used time-lapse imaging analysis with or without tPA and tPA stop (Fig. 2e). NPCs were plated at a density of 20,000 cells/cm^2 and exposed to tPA, tPA stop, or tPA/tPA stop. Images were captured at every 30 min intervals up to 72 h (refer to "Materials and Methods"). tPA increased the branch number and length of neurites from NPCs but co-incubation of tPA stop with tPA abrogated the increased neurite outgrowth (Fig. 2e). Blocking of endogenous tPA activity with tPA stop inhibited neurite outgrowth in time-lapse microscopy compared with vehicle-treated controls (Fig. 2e).

To investigate the effect of overexpression of tPA in neurite outgrowth in NPCs, we transfected NPCs with tPA-GFP. Differentiation of NPCs was induced for 3 days following transfection. tPA-GFP-transfected cells showed higher branch number (Fig. 2f; 2.35±0.25 vs 4.23±0.42) and longer neurite length (19.68±1.69 vs 33.73±2.99 μm) compared with GFP-transfected cells (Fig. 2g).

We next knocked down the expression of endogenous tPA in NPCs via transient transfection with tPA siRNA as described in the "Materials and Methods." The knockdown of tPA expression by tPA siRNA transfection was confirmed by RT-PCR, Western blot, and zymography (Fig. 2g). The transfected cells were differentiated for 3 days and tPA siRNA-transfected NPCs showed lower branch number and shorter neurite length compared to mock controls or control siRNA-transfected NPCs (Fig. 2h). In addition, expressions of neuronal markers such as Tuj-1, GAD, PSD-95, and synaptophysin were decreased by tPA siRNA transfection as determined by Western blot (Fig. 2i).

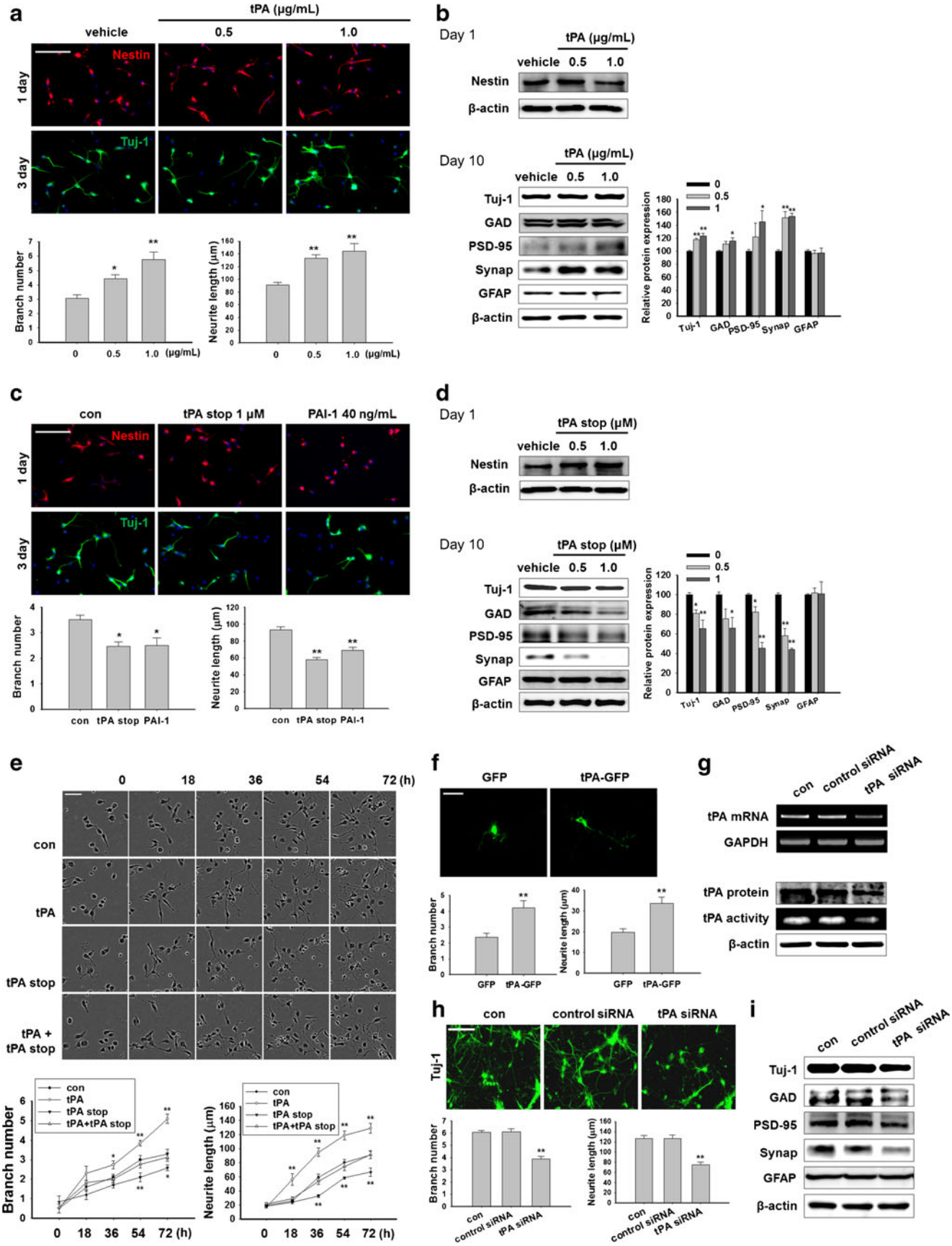
a
tPA (μg/mL)
vehicle
0.5
1.0
Nestin
Tuj-1
1 day
3 day
Branch number
Neurite length (μm)
0
0.5
1.0 (μg/mL)
b
Day 1
tPA (μg/mL)
vehicle 0.5 1.0
Nestin
β-actin
Day 10
Tuj-1
GAD
PSD-95
Synap
GFAP
Relative protein expression
c
con
tPA stop 1 μM
PAI-1 40 ng/mL
con tPA stop PAI-1
d
tPA stop (μM)
e
0 18 36 54 72 (h)
con
tPA
tPA stop
tPA + tPA stop
tPA+tPA stop
f
GFP
tPA-GFP
g
con control siRNA tPA siRNA
tPA mRNA
GAPDH
tPA protein
tPA activity
h
control siRNA
tPA siRNA
i

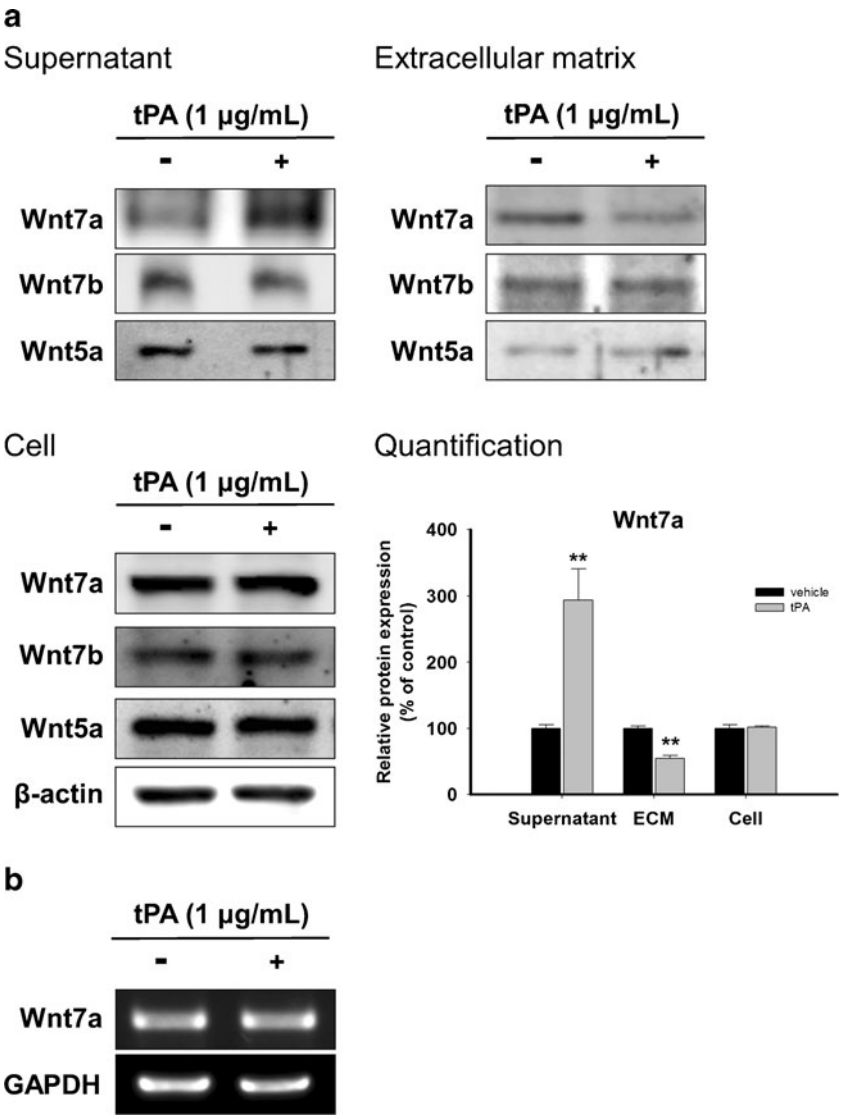

Fig. 3 tPA increased Wnt7a release from extracellular matrix (ECM). **a** NPCs were washed and incubated for 6 h with tPA (1 μg/ml). Supernatants containing released proteins were collected and cells were detached from ECM with 1 mM EDTA and then harvested. After detachment of cells from ECM, ECM proteins were extracted with 2× SDS-PAGE sample loading buffer. Each fraction was analyzed for Wnt subtype contents by Western blot. Values represent mean ± SEM (Student's *t* test, $^{**}p<0.01$, $n=3$). **b** Expression of Wnt7a mRNA was analyzed 6 h after tPA treatment. GAPDH was used as a loading control

We next investigated the involvement of the Wnt signaling pathway in tPA-induced neurite outgrowth in NPCs. First, we collected the supernatant from NPCs after tPA treatment and the level of several subtypes of Wnt was analyzed by Western blot. Among the several Wnt subtypes that may be involved in the increase of neurite outgrowth, the release of Wnt7a into the culture supernatant was reliably increased 2 h after tPA treatment with a concomitant decrease of Wnt7a associated with ECM (Fig. 3a). However, other Wnt subtypes such as Wnt5a and 7b were not significantly affected by tPA (Fig. 3a). In addition, Wnt1 was not affected by tPA and Wnt3a was not reliably detected in culture supernatants (data not shown). Interestingly, the cellular level of Wnt7a (Fig. 3a) nor its mRNA expression was significantly affected by tPA (Fig. 3b), suggesting that tPA increases the release of Wnt7a from ECM but does not upregulate Wnt7a expression.

To check the hypothesis that tPA may directly bind to LRP5/6 and induce phosphorylation of LRP5/6, we performed co-immunoprecipitation experiments using tPA antibody. When NPC lysates were immunoprecipitated with tPA antibody, we detected LRP5 immunoreactivity as well as tPA immunoreactivity in immunoprecipitates (Fig. 4a). Similar co-immunoprecipitation of LPR6 with tPA was also observed (data not shown). Unfortunately, both LRP5 and LRP6 antibodies were not suitable for immunoprecipitation experiments, so we conducted crosslinking experiments to confirm the physical association of tPA with LRP5/6 (refer to "Materials and Methods") [40]. After crosslinking of closely interacting molecules with DTSSP, immunoprecipitation was conducted with tPA. During the SDS-PAGE process, linked molecules were disconnected, thereby providing information about the closely interacting proteins after Western blot [40]. Consistent with the results obtained from the co-immunoprecipitation

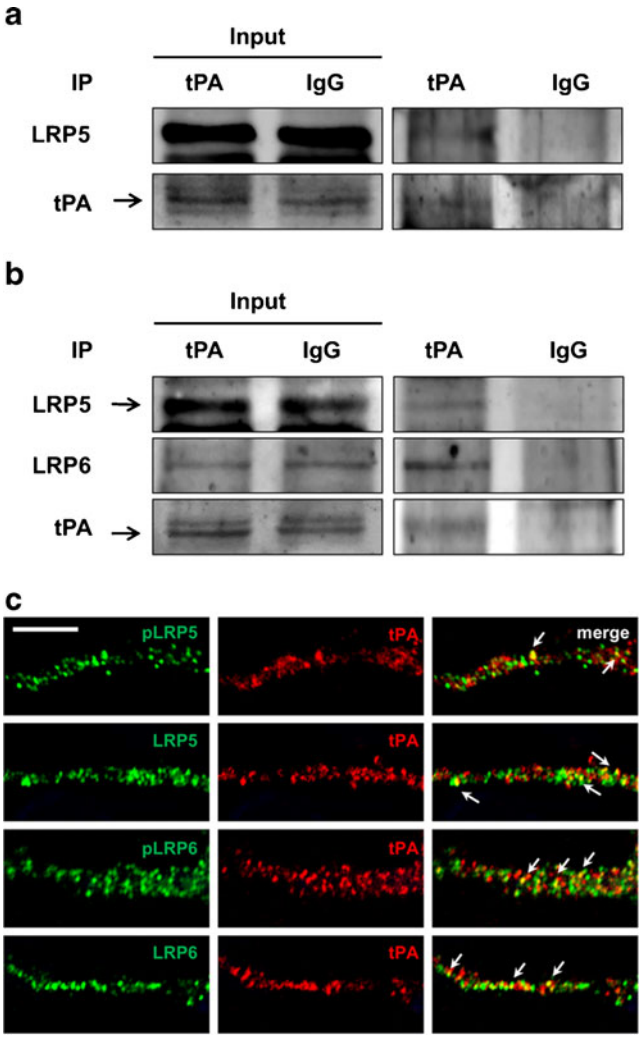

Fig. 4 tPA binds to LRP5/6. **a** Co-immunoprecipitation of endogenous tPA and LRP5/6 in NPCs. Cell lysates (700 μg) were incubated with tPA antibody (2 μg) and the immunoprecipitates were analyzed by Western blot. **b** Crosslinking and co-immunoprecipitation of endogenous tPA and LRP5/6 in NPCs. Crosslinking of tPA and LRP5/6 was conducted as described in "Materials and Methods." **c** Colocalization of tPA with pLRP5, LRP5, pLRP6, or LRP6 in NPC processes. NPCs were cultured in the differentiation condition for 24 h and stained with the indicated antibodies. *Arrows* indicate colocalization of tPA and LRP5/6. Scale bar=2 μm

experiments, LRP5/6 was co-immunoprecipitated with tPA after crosslinking (Fig. 4b). We performed an immunocytochemistry which showed a colocalization of LRP5/6 and pLRP5/6 with tPA in NPC processes (Fig. 4c, arrows).

In the Wnt signaling pathway, phosphorylation of LRP5/6 plays an important role in the regulation of GSK3β phosphorylation and stabilization of β-catenin [43, 44]. As shown in Fig. 5a, treatment of NPCs with tPA rapidly induced phosphorylation of LRP5/6 and GSK3β as well as induction of the level of β-catenin in a time- and concentration-dependent manner. The total level of LRP5/6 and GSK3β was not significantly changed by tPA. Quantification of the data showed that phosphorylation of LRP5/6 was significantly upregulated as quickly as 5 min after tPA treatment followed by an increase in phosphorylation of GSK3β and upregulation of β-catenin (Fig. 5b), which suggests that tPA activates the Wnt–LRP5/6–GSK3β–β-catenin pathway in cultured NPCs.

It is known that β-catenin is localized in growth cones of developing hippocampal neurons and regulates cytoskeletal organization [45]. Therefore, we next checked localization of β-catenin at tips of NPC processes after tPA treatment. As shown in Fig. 5c, β-catenin was upregulated at process tips of Nestin-positive NPCs at 6 and 24 h after tPA treatment.

We next investigated the effects of tPA knockdown on LRP5/6 signaling in NPCs. NPCs were transiently transfected with tPA siRNA as in Fig. 2. As shown in Fig. 6a, Western blot revealed that phosphorylation of LRP5/6 and GSK3β as well as accumulation of β-catenin was decreased by tPA siRNA transfection in NPCs. In addition, immunocytochemical localization of β-catenin in NPC process tips was decreased by tPA siRNA transfection (Fig. 6b).

To further investigate the involvement of LRP5/6 in tPA-induced regulation of GSK3β phosphorylation and β-catenin accumulation, NPCs were transfected with LRP5/6 siRNA. The endogenous level of LRP5/6 and pLRP5/6 was knocked down by cognate siRNA transfection in NPCs (Fig. 7a). In this condition, phosphorylation of GSK3β and accumulation of β-catenin were also decreased (Fig. 7a). Next, we stimulated LRP5 or LRP6 siRNA-transfected NPCs with tPA for 30 min. After stimulation, Western blot analysis showed that increased phosphorylation of GSK3β and upregulation of β-catenin by tPA were prevented by LRP5/6 siRNA transfection (Fig. 7b). The expression of total GSK3β and β-actin was similar in all samples, which was used as a loading control. Likewise, immunocytochemical staining showed that tPA-induced increase of β-catenin accumulation in NPC tips was inhibited by LRP5/6 siRNA transfection (Fig. 7c). When NPCs were allowed to differentiate for 3 days, tPA-induced neurite outgrowth was inhibited by LRP5/6 siRNA transfection (Fig. 7d). These results suggest that tPA increased neurite outgrowth in NPCs via phosphorylation of LRP5/6 in NPCs.

To further demonstrate that the increase of neurite outgrowth by tPA is mediated by the pGSK3β and the β-catenin pathways, we first investigated neurite outgrowth after transfection of GSK3β mutants. S9A is a constitutively active GSK mutant which causes downregulation of β-catenin. K85A is a kinase dead GSK mutant which causes an upregulation of β-catenin. Transfected cells were shown as green fluorescence by cotransfection of GFP. In cells transfected with GFP alone, tPA increased neurite outgrowth; however, the increased neurite outgrowth was blocked by WT and S9A GSK transfection (Fig. 8a). Notably, neurite outgrowth was increased by K85A transfection even without tPA treatment, which suggests

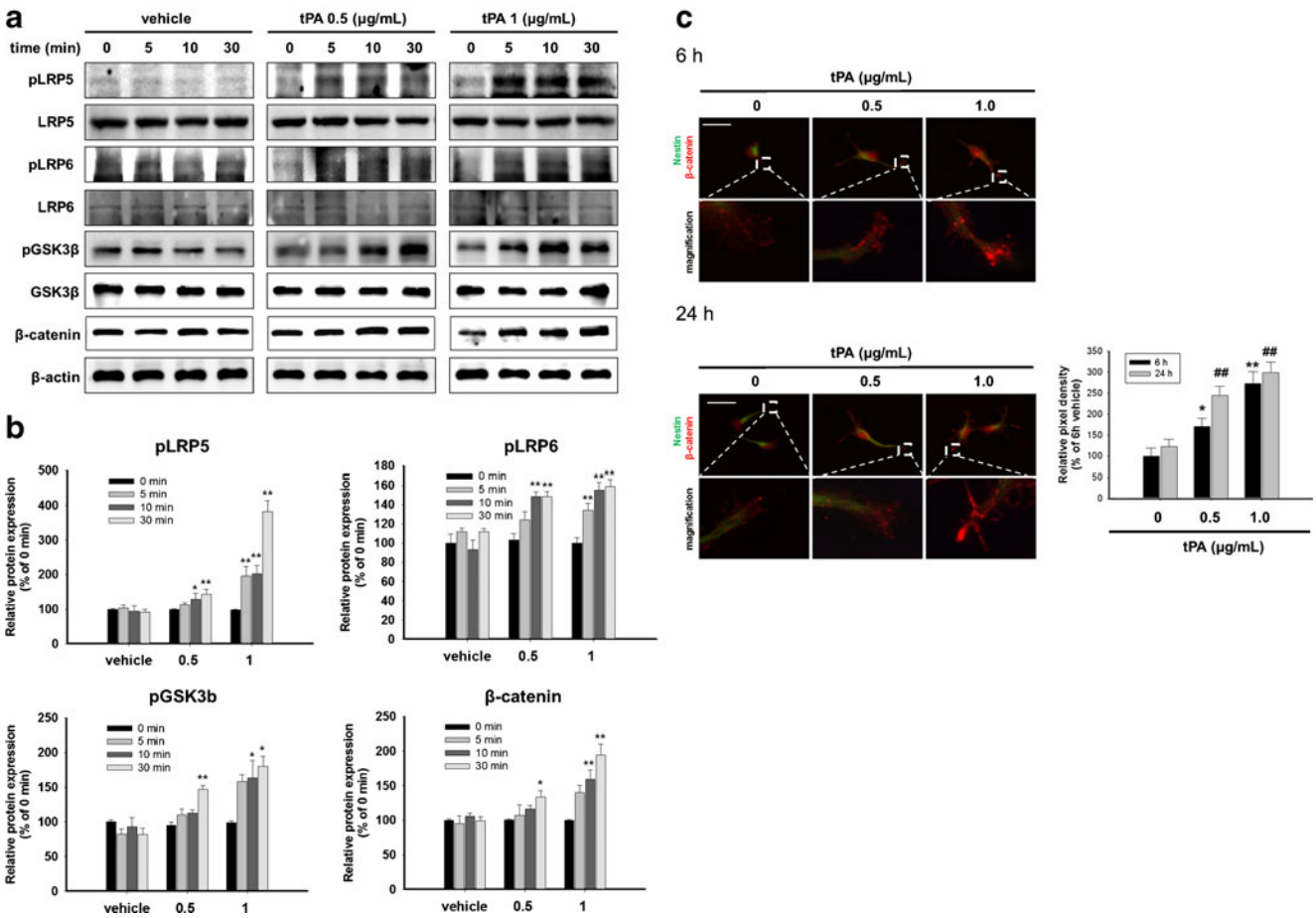

Fig. 5 tPA increased phosphorylation of LRP5/6 and GSK3β and accumulation of β-catenin. **a**, **b** NPCs were incubated with 0.5 and 1 μg/ml of tPA and harvested at each time point. Total and phosphorylated LRP5/6 and GSK3β as well as β-catenin were analyzed by Western blot. *$p<0.05$, **$p<0.01$ (one-way ANOVA, $n=5$). **c** NPCs were fixed 6 and 24 h after tPA application (1 μg/ml) and immunostained for β-catenin at the tips of NPC processes. In each cover slip, 20 cells were randomly selected and analyzed. Scale bar=20 μm. *$p<0.05$, **$p<0.01$ (one-way ANOVA, $n=3$)

that tPA-mediated neurite outgrowth is dependent on the phosphorylation-induced inactivation of kinase activity of GSK3β. In K85A-transfected NPCs, tPA did not further augment neurite outgrowth.

We also investigated neurite outgrowth by tPA in NPC cells in which the endogenous β-catenin level was knocked down by β-catenin siRNA transfection (Fig. 8b). In NPCs transfected with β-catenin siRNA, tPA failed to induce neurite outgrowth (Fig. 8c), suggesting that tPA-induced neurite outgrowth is dependent on β-catenin upregulation.

We next investigated the level of LRP5/6–GSK3β–β-catenin signaling activity in tPA KO mice. NPCs were isolated from the cortical region of the E12.5 embryonic brain of tPA KO and WT mice (refer to "Materials and Methods"). On day 1 after induction of differentiation, the levels of pLRP5/6, pGSK3β, and β-catenin were lower in NPCs derived from tPA KO compared with WT. Furthermore, addition of exogenous tPA (1 μg/ml) partially increased the decreased level of pLRP5/6–GSK3β–β-catenin (Fig. 9b). These results suggest that the absence of tPA activity in NPCs from tPA KO mice adversely affected the pLRP5/6–GSK3β–β-catenin signaling pathway. As expected, immunocytochemistry data also showed that neurite outgrowth was reduced until day 4 in NPCs derived from tPA KO compared to WT, and the decreased neurite outgrowth was partially recovered by exogenous addition of tPA (Fig. 9c). Interestingly, no significant difference was observed in neurite outgrowth between NPCs derived from WT and tPA KO mice at day 7 (data not shown), suggesting the involvement of compensatory mechanisms to catch up the aberrant neurite outgrowth in NPCs from tPA KO mice (Fig. 9c).

Finally, to determine the role of tPA-induced neurite outgrowth from NPCs in pathological conditions in vivo, neurite outgrowth was investigated in the MCAO-damaged brain after transplantation of NPCs derived from WT and tPA KO mice. Mouse embryonic NPCs from WT and tPA KO mice were transplanted into the striatum after MCAO as described in "Materials and Methods." Sham-operated

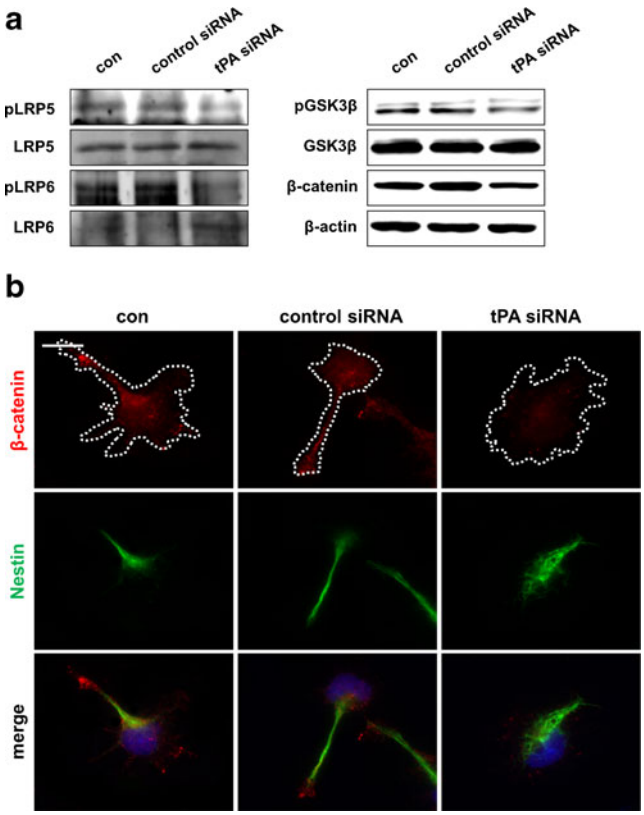

Fig. 6 Phosphorylation of LRP5/6 is inhibited by knockdown of endogenous tPA expression. **a** NPCs were transfected with tPA siRNA (100 pmol) as described in "Materials and Methods." The transfected NPCs were harvested 24 h after transfection. Total and phosphorylated LRP5/6, GSK3β, and β-catenin were analyzed by Western blot. **b** NPCs were transfected with tPA siRNA for 24 h and fixed for immunostaining against β-catenin and Nestin. Cell nuclei were counterstained with DAPI. Scale bar=10 μm

control (no MCAO) or vehicle-treated control (MCAO without NPCs transplantation) animals were injected with the same volume of the culture medium. Rats were sacrificed 2 weeks after transplantation and brains were subjected to Bielshowsky silver and Luxol fast blue staining to visualize axons and myelins. Quantification of axon density and fiber length was performed with MCIDTM analysis (Micro Computer Imaging Device) (Imaging Research, St. Catharines, Ontario, Canada). MCAO decreased axon density in the striatum and the damaged axon was partially recovered by transplantation of WT NPCs (Fig. 10; axon density 53.13±6.35 % and 80.91±4.34 %) compared with controls (sham MCAO group) in MCAO-Vehicle and MCAO-WT, respectively (fiber length 55.55±6.73 and 80.54±6.56 % in MCAO-Vehicle and MCAO-WT, respectively). However, transplantation of NPCs obtained from tPA KO mice failed to induce neurite outgrowth (axon density 50.03±6.60 %, fiber length 53.88±4.50 % compared with control). These results suggest that tPA expression in transplanted NPCs regulates neurite outgrowth in the MCAO-damaged brain.

Discussion

In this study, we provided evidence that tPA expressed in NPCs induces neurite outgrowth during differentiation of NPCs into neurons through activation of the Wnt–LRP5/6–GSK3β–β-catenin signaling pathway. In cultured NPCs, tPA induced neurite outgrowth by increased release of Wnt7a and direct binding of tPA to LRP5/6, both of which contributed to increased phosphorylation of LRP5/6 and Wnt downstream signaling.

The role of Wnt7a in growth cone spreading in developing cerebellar granule neurons has been reported [10, 46], which was mimicked by GSK3β inhibitors such as LiCl and valproic acid, possibly via regulation of microtubule stabilization [47]. These results suggest that Wnt7a regulates microtubule stabilization by the regulation of GSK3β [47]. Interestingly, Wnt7a intracellular signaling is modulated by LRP6 in PC12 cells [48].

Extracellular matrix components, especially glycosaminoglycan (GAG) polysaccharides, such as heparan sulfate and chondroitin sulfate, bind many proteins including growth factors, chemokines, and neuromodulators and sequester them until they are released again into the extracellular space. Although proteins that bind to GAG are protected from proteolysis in general, proteinase may release proteins by cleaving ECM molecules. Plasmin has been suggested to release guidance molecules F-spondin [49] and VEGF [50] from ECM. Interestingly, tPA also binds to GAG in addition to Wnt [51]. These reports suggest that tPA may increase Wnt7a in the extracellular space either by competitively replacing its binding to GAG or by releasing it from ECM through its proteolytic action, although these possibilities should be experimentally verified in the future.

LRP-1, a receptor which mediates signaling events by tPA, was reported to increase neurite outgrowth in PC12 cells and rat primary cortical neurons through transactivation of Trk and activation of CREB by the MAPK pathway [23, 24]. In this study, although we can detect the expression of LRP-1 in rat NPCs, phosphorylation of LRP-1 was under the detection limit and tPA did not induce activation of the MAPK or Akt pathway (data not shown). In contrast to Wnt activation by LRP5/6, it is reported that LRP-1 downregulates the Wnt pathway by sequestering Frizzled in 293 T cells [52]. Furthermore, β-catenin was decreased by LRP-1 overexpression in chondrocytes [53]. Similarly, a LRP-1 ligand α2-macroglobulin inhibits the Wnt–β-catenin pathway in 1321 N1 astrocytoma cells [54]. All together, these results suggest that LRP-1 is not a major target of tPA-mediated Wnt–GSK3β–β-catenin-dependent neurite outgrowth in rat primary NPCs.

Several researchers reported the essential role of LRP5/6 in embryonic and neuronal development. In LRP5 mutant mice, defective development of retinal vasculatures was

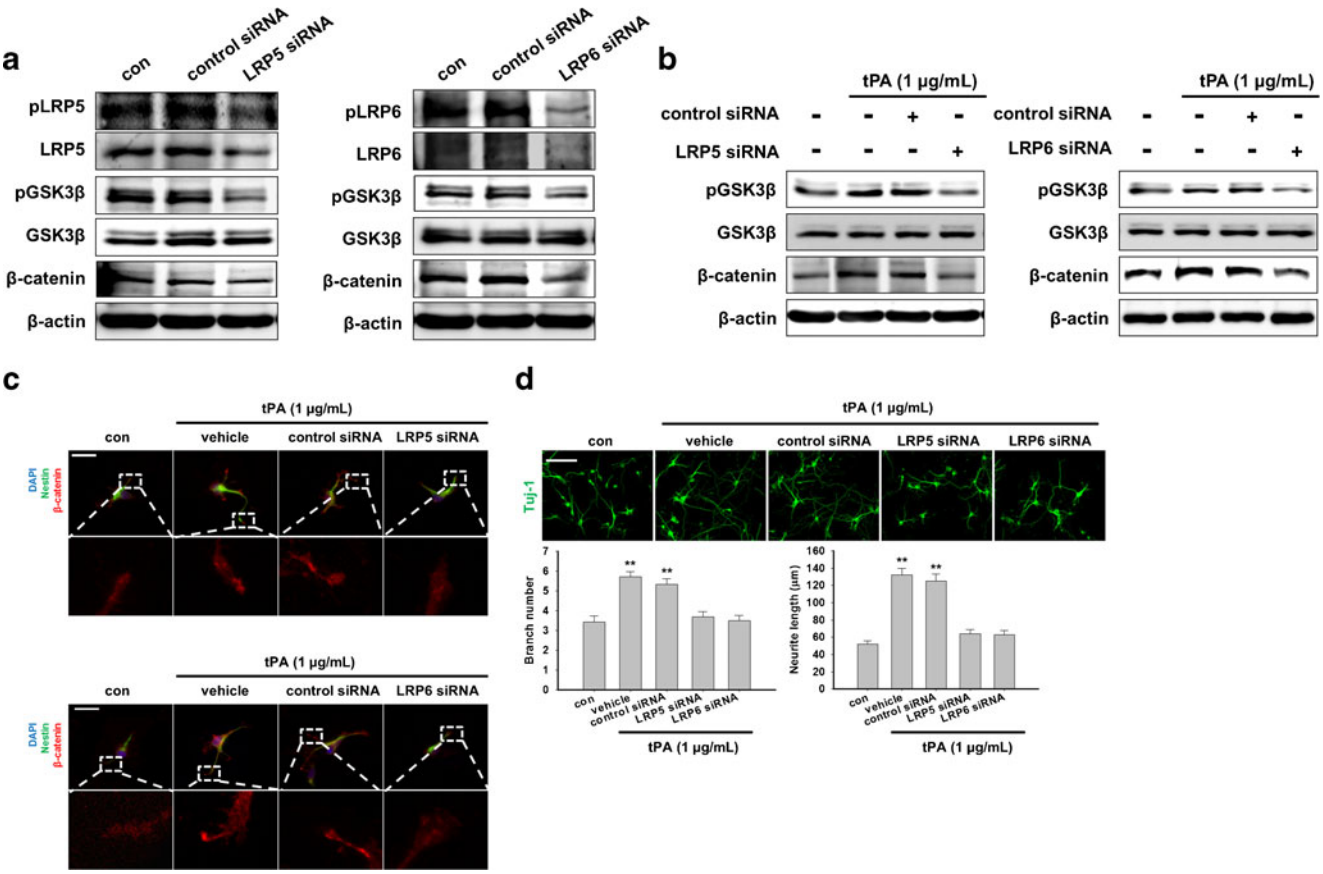

Fig. 7 tPA induces phosphorylation of GSK3β and accumulation of β-catenin through LRP5/6. **a** NPCs were transfected with LRP5 or LRP6 siRNA (100 pmol) as described in "Materials and Methods." The cells were harvested 24 h after transfection. Total GSK3β and β-actin were used as loading controls. **b**, **c** LRP5 or LRP6 siRNA-transfected cells were incubated with tPA (1 μg/ml) for 30 min at 37 °C and harvested or fixed for further analysis by Western blot (**b**) and immunocytochemistry for β-catenin (**c**). Scale bar=10 μm. **d** Transfected NPCs were incubated in the presence or absence of tPA for 3 days and immunostained against Tuj-1 for the analysis of neurite outgrowth. Scale bar=100 μm. More than 20 cells were analyzed in each of the three experiments. Values represent mean ± SEM (Student's *t* test, $*p<0.05$, $**p<0.01$, $n=3$)

reported which was caused by the decrease of sprouting in vascular endothelial cells [55]. LRP6−/− embryo shows severe defects in the midbrain, hindbrain, and limb development [17] as well as delayed dopaminergic neuronal differentiation [56]. Of note, the defective limb patterning in LRP6 mutant mice was similar to that in Wnt7a mutant mice, suggesting a functional link between the two molecules [57, 58].

In our study, tPA increased neurite outgrowth, which is related to the increase of β-catenin in the tips of differentiating NPC processes by inhibition of GSK3β activity. Although conflicting results exist regarding the role of GSK3β in controlling axonal outgrowth, it is reported that different responses of neurite outgrowth are dependent on the intensity of GSK3β inhibition [59]. A previous report showed that tPA mediates epidermal growth factor receptor transactivation-induced rapid accumulation of β-catenin in ECV 304 carcinomca cells [12]. In depolarized hippocampal neurons, it has been suggested that β-catenin regulates dendritic morphogenesis through interaction with N-cadherin [60]. In this case, Wnt-mediated stabilization of β-catenin increased dendritic growth and arborization, which are independent of transcriptional activation, suggesting that local accumulation of β-catenin rather than transcriptional activation of downstream target molecules is the most important in the regulation of neurite outgrowth at least in the initial stage of growth.

In this study, the expression level of β-catenin was reduced in NPCs derived from tPA KO mice at day 1, whereas no significant difference was observed in the level of β-catenin at day 7, which is consistent with the delayed but otherwise normal neurite outgrowth compared to WT. In this study, the delayed neurite outgrowth in NPCs derived from tPA KO mice was normalized at later time points of differentiation such as day 7 or 10, suggesting that NPCs are equipped with compensatory mechanisms to cope with the absence of tPA. In addition to tPA, it has been reported that uPA and uPA receptor (uPAR) may be involved in the regulation of neurite outgrowth [61, 62]. In addition, overexpression of uPAR upregulated Wnt7a–β-catenin signaling in medulloblastoma cells [63]. Interestingly, it has been suggested that uPA may

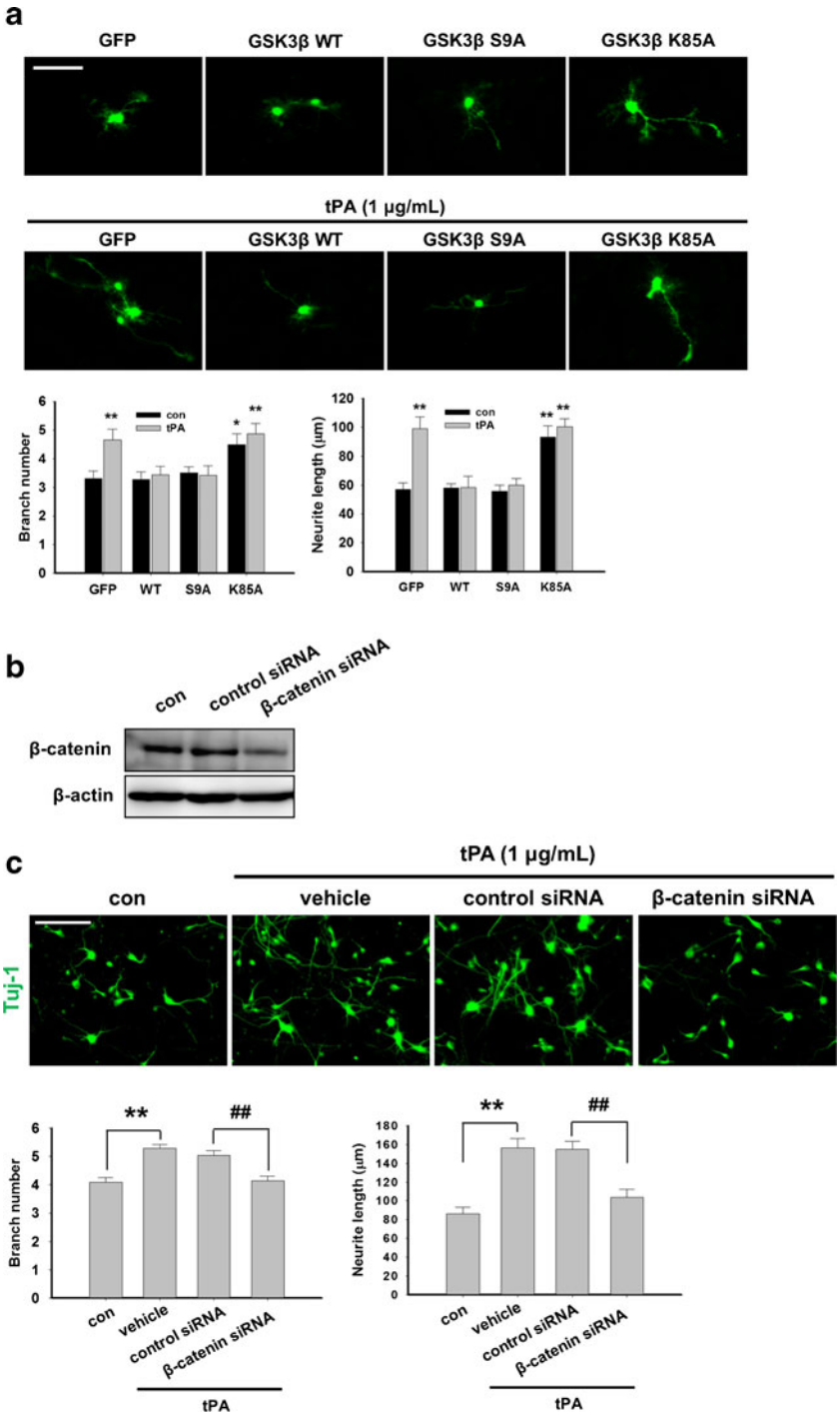

Fig. 8 tPA-induced neurite outgrowth is dependent on the modulation of GSK3β activity and β-catenin accumulation. **a** NPCs were cotransfected with GFP and GSK3β WT, S9A, and K85A. Transfected NPCs were incubated with tPA (1 μg/ml), and the cells were allowed to differentiate for 3 days and were fixed for neurite outgrowth analysis. Scale bar=50 μm. *$p<0.05$, **$p<0.01$ (Student's t test, $n=3$). **b** NPCs were transfected with β-catenin siRNA and were harvested 24 h after transfection for Western blot analysis. **c** NPCs transfected with β-catenin siRNA were treated with tPA and then differentiated for 3 days. The cells were immunostained with Tuj-1 for analysis of neurite outgrowth. Scale bar=100 μm. Values represent the mean of three determinations ± SEM (Student's t test, **$p<0.01$, compared to control; ##$p<0.01$, compared to control siRNA, $n=3$)

compensate for the loss of tPA in tPA KO mice and results in the augmentation of plasmin activity [64]. In addition to uPA, the possibilities of upregulation of other proteinases such as MMPs or growth factors and their role on the regulation of neurite outgrowth should be further investigated in the future to obtain a comprehensive understanding of the kinetic profile of neurite outgrowth in tPA KO NPCs.

Even though the defects in neurite outgrowth in tPA KO mice were overcome at later time points in culture, the delayed neurite outgrowth may affect migration, integration, and regeneration of neurons during development and under neurotraumatic conditions. It is reported that axonal outgrowth is essential for granular precursor cell migration and inhibition of neurite outgrowth by blocking MMP9 activity results in aberrant granular precursor cell numbers in the external granular layer of the cerebellum [65, 66]. TrkB−/− neocortical neurons showed delayed neurite outgrowth in vitro and reduced integration after transplantation in the developing neocortex [67]. In matrilin-2-deficient mice,

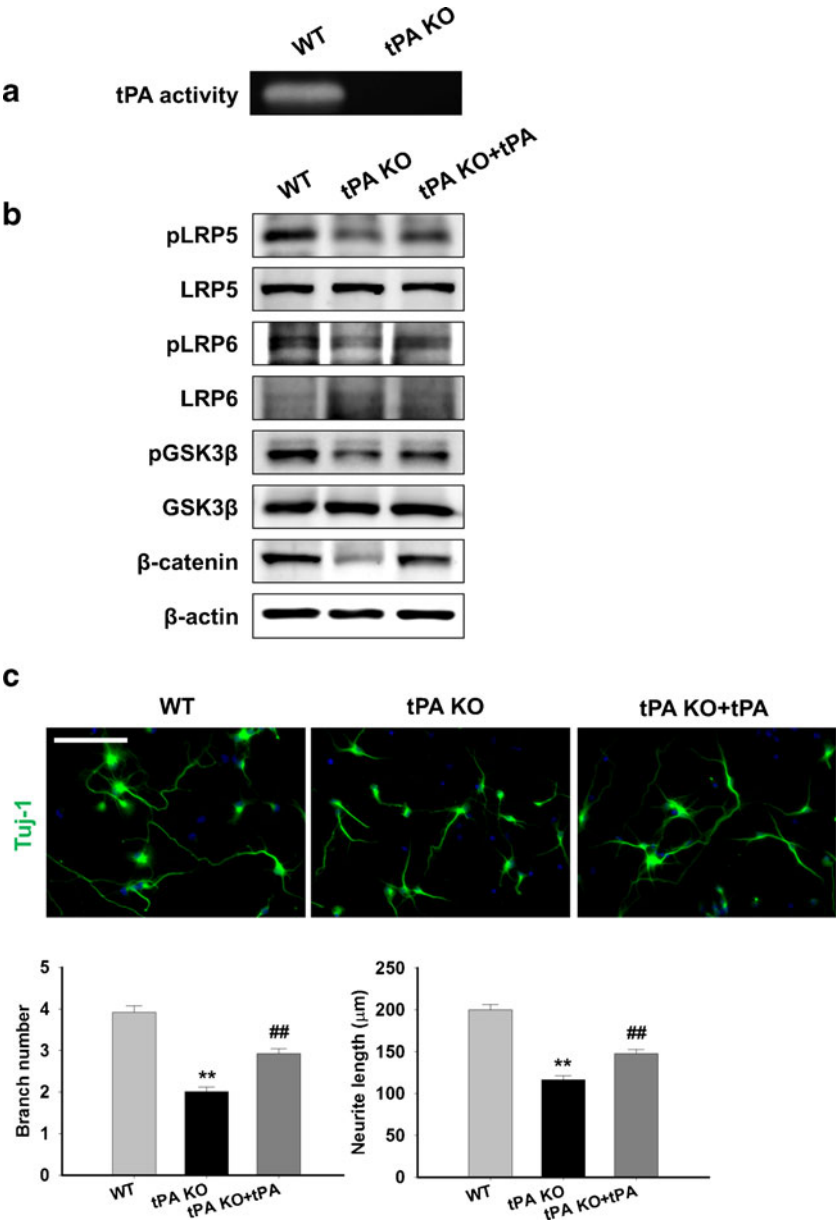

Fig. 9 NPCs from tPA KO mice showed delayed neurite outgrowth. **a** Mice embryonic NPCs were isolated from E12.5 embryo of WT and tPA KO mice. Zymographic activity of tPA was shown in WT but not in tPA KO NPCs. **b** Exogenous tPA (1 μg/ml) was added to NPCs from tPA KO and NPCs were harvested at day 1. Expressions of pLRP5/6, pGSK3β, and β-catenin were examined by Western blot. β-Actin was used as a loading control. **c** Cultured NPCs were differentiated for 4 days and immunostained against Tuj-1 for analysis of neurite outgrowth. In each cover slip, more than 50 cells were randomly selected and analyzed. Scale bar=100 μm. Values represent mean ± SEM (Student's *t* test, $^{**}p<0.01$, compared to WT; $\#\#p<0.01$, compared to tPA KO, $n=3$)

axonal outgrowth from dorsal root ganglia neurons was decreased, which resulted in delayed motor recovery and regeneration after a femoral nerve lesion [68]. In tPA KO mice, time-lapse microscopy revealed that the speed of migration of cerebellar granule neurons was reduced, which resulted in defects in the developing granular layer [69]. In addition, tPA KO mice showed abnormal mossy fiber outgrowth in the hippocampus after short seizure episodes, suggesting aberrant axonal pathfinding in tPA KO mice [2]. In this study, the increase in neurite outgrowth by tPA is already evident in Nestin-positive cells that are devoid of strong Tuj-1 immunoreactivity. This suggests that tPA acts very early to regulate neurite outgrowth during the development of neurons from NPCs. tPA not only increased the length of neurites but also increased the expression of synaptic proteins, especially synaptophysin, suggesting that tPA may also take part in the modulation of functional maturation of synapse which might be related to the well-documented role of tPA in the regulation of synaptic plasticity.

In this study, exogenous addition of tPA partially recovered the decreased protein expression of pLRP5/6, GSK3β, and β-catenin as well as neurite outgrowth in NPCs from tPA KO mice, suggesting the essential role of tPA in the regulation of Wnt signaling in NPCs. In addition, transplantation of NPCs obtained from WT but not tPA KO mice partially recovered the damaged axon, suggesting that tPA in NPCs play an important role in neuronal regeneration in pathological conditions. Recently, it has been suggested that transplantation of multipotent mesenchymal stromal cells increased neurite outgrowth in the MCAO-induced ischemic brain [5, 70]. Transplantation of mesenchymal stromal cells

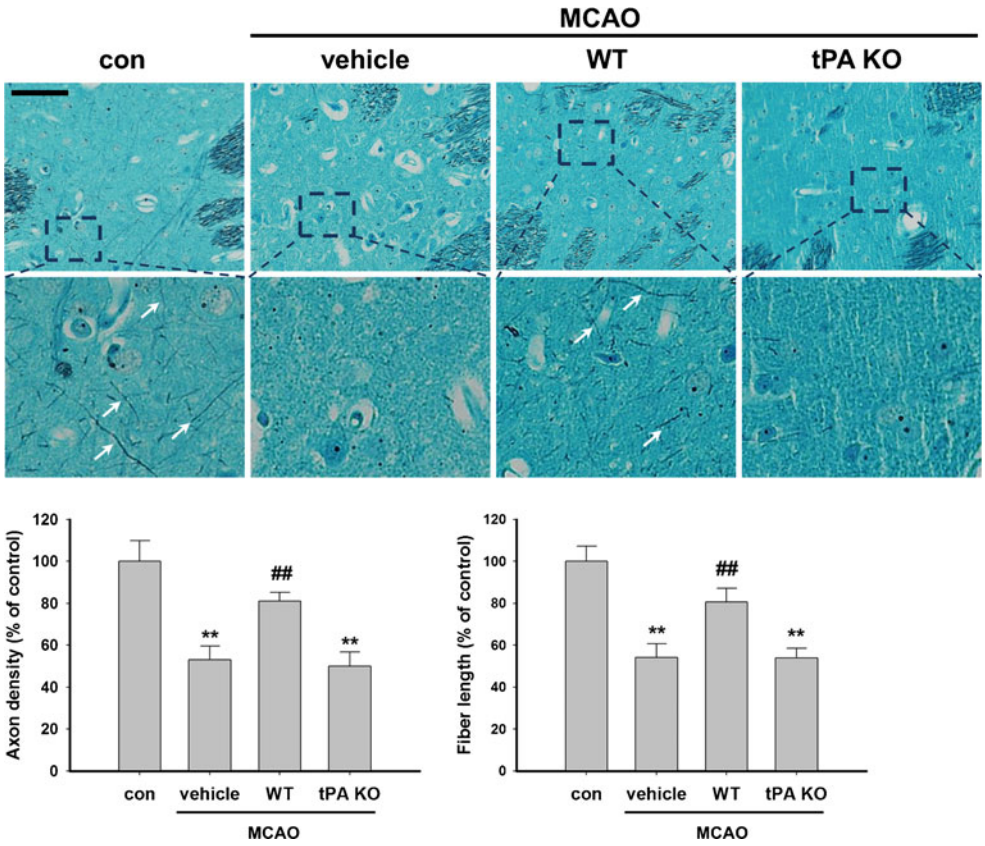

Fig. 10 Transplantation of tPA KO NPCs failed to induce neurite outgrowth in MCAO-damaged brain. NPCs were isolated from embryonic brains of WT or tPA KO mice. NPCs were transplanted into the MCAO-damaged rat striatum as described in "Materials and Methods." Rats were sacrificed 2 weeks after transplantation for Bielschowsky and Luxol fast blue staining. *Arrows* indicate axonal staining which appear as *black lines*. Axonal outgrowth was obvious in WT but not in the tPA KO NPC-transplanted brain. In each sample, nine microscopic fields were randomly selected and analyzed for axonal stain density as well as the length of individual stained axon. Scale bar=100 μm. Values represent mean ± SEM (Student's *t* test, $^{**}p<0.01$, compared to control; $^{\#\#}p<0.01$, compared to vehicle, $n=6$)

did not induce neurite outgrowth in tPA KO mice, and this suggests that the transplantation of mesenchymal stem cells regulates neurite regeneration indirectly by regulating endogenous tPA from neurons and astrocytes [5, 70]. In our experiment, NPCs obtained from tPA KO mice did not provide increased neurite extension, which indicated a more direct role of tPA originating from NPCs tPA in the regulation of neurite extension in the injured brain. However, it is still possible that NPCs also provide increased release of endogenous tPA or induce trophic support such as BDNF [71], GDNF [72], VEGF, and neutrophin-3 [73]. Although we showed reduced neurite outgrowth in ischemic brain transplanted with NPCs obtained from tPA KO mice, it is essential to determine whether transplantation of NPCs from WT or tPA KO mice differentially affects neuronal degeneration/regeneration in terms of the extent of tissue damage and functional recovery. In this regard, experimental conditions should be carefully adjusted to see the general differences in tissue damage/regeneration as a whole, which is detectible by conventional methods such as TTC staining. For example, the optimal cell number of NPCs for transplantation, the injection of NPCs in multiple sites, ideal injection time windows, and many other experimental variables should be carefully determined in a future study.

In conclusion, we report here that tPA expressed in NPCs regulates neuronal development and regeneration by inducing neurite outgrowth via the Wnt–LRP5/6 pathway, which might provide a new target to regulate neurite extension during development as well as neurological insult conditions such as stroke. Considering the diverse role of the Wnt–LRP5/6 pathway in a myriad of physiological and pathological processes in many cell types including cancer cells, understanding the exact mechanism by which tPA modulates this signaling pathway may provide additional impetus to an already intriguing study of the proteinase.

Summary

In CNS, tPA plays an important neuromodulatory role including regulation of cell death, neuronal migration, and neurite extension. We found here that tPA is expressed in rat NPCs. tPA in NPCs induced neurite extension via mechanism involving increased GSK3β–β-catenin signal that was mediated by increased Wnt7a release and phosphorylation of LRP5/6. In due course of the experiments, we provided the first experimental evidence that tPA physically interacts with LRP5/6 and induces phosphorylation, which may have wide implication in the regulation of neural processes from differentiation to the regulation of synaptic plasticity. Using NPC culture derived from tPA KO mice, we showed aberrant neurite extension in tPA-deficient cultured

NPCs. In addition, NPCs derived from tPA KO mice failed to induce neurite extension when they are transplanted in ischemic brain. The expression of tPA in NPCs would be a new target for the regulation of neural development or regeneration.

Acknowledgments This work was supported by a grant of the Korean Health Technology R&D Project, Ministry of Health & Welfare, Republic of Korea (No. A120029), and by the Mid-career Researcher Program Project No. 2011–0014258 through the National Research Foundation of Korea (NRF) grant funded by the Korea Government (MEST) (Shin, C.Y.).

Conflict of Interest The authors declare no conflict of interest or competing commercial interests.

References

1. Pittman RN, Ivins JK, Buettner HM (1989) Neuronal plasminogen activators: cell surface binding sites and involvement in neurite outgrowth. J Neurosci 9:4269–4286
2. Wu YP, Siao CJ, Lu W, Sung TC, Frohman MA et al (2000) The tissue plasminogen activator (tPA)/plasmin extracellular proteolytic system regulates seizure-induced hippocampal mossy fiber outgrowth through a proteoglycan substrate. J Cell Biol 148:1295–1304
3. Verrall S, Seeds NW (1989) Characterization of 125I-tissue plasminogen activator binding to cerebellar granule neurons. J Cell Biol 109:265–271
4. Jacovina AT, Zhong F, Khazanova E, Lev E, Deora AB et al (2001) Neuritogenesis and the nerve growth factor-induced differentiation of PC-12 cells requires annexin II-mediated plasmin generation. J Biol Chem 276:49350–49358
5. Shen LH, Xin H, Li Y, Zhang RL, Cui Y et al (2011) Endogenous tissue plasminogen activator mediates bone marrow stromal cell-induced neurite remodeling after stroke in mice. Stroke 42:459–464
6. Siconolfi LB, Seeds NW (2001) Induction of the plasminogen activator system accompanies peripheral nerve regeneration after sciatic nerve crush. J Neurosci 21:4336–4347
7. Siconolfi LB, Seeds NW (2001) Mice lacking tPA, uPA, or plasminogen genes showed delayed functional recovery after sciatic nerve crush. J Neurosci 21:4348–4355
8. Akiyama T (2000) Wnt/beta-catenin signaling. Cytokine Growth Factor Rev 11:273–282
9. Fradkin LG, Noordermeer JN, Nusse R (1995) The Drosophila Wnt protein DWnt-3 is a secreted glycoprotein localized on the axon tracts of the embryonic CNS. Dev Biol 168:202–213
10. Hall AC, Lucas FR, Salinas PC (2000) Axonal remodeling and synaptic differentiation in the cerebellum is regulated by WNT-7a signaling. Cell 100:525–535
11. Purro SA, Ciani L, Hoyos-Flight M, Stamatakou E, Siomou E et al (2008) Wnt regulates axon behavior through changes in microtubule growth directionality: a new role for adenomatous polyposis coli. J Neurosci 28:8644–8654
12. Maupas-Schwalm F, Robinet C, Auge N, Thiers JC, Garcia V et al (2005) Activation of the {beta}-catenin/T-cell-specific transcription factor/lymphoid enhancer factor-1 pathway by plasminogen activators in ECV304 carcinoma cells. Cancer Res 65:526–532
13. Lin L, Bu G, Mars WM, Reeves WB, Tanaka S et al (2010) tPA activates LDL receptor-related protein 1-mediated mitogenic signaling involving the p90RSK and GSK3beta pathway. Am J Pathol 177:1687–1696
14. Rulifson EJ, Wu CH, Nusse R (2000) Pathway specificity by the bifunctional receptor frizzled is determined by affinity for wingless. Mol Cell 6:117–126
15. Bhanot P, Fish M, Jemison JA, Nusse R, Nathans J et al (1999) Frizzled and Dfrizzled-2 function as redundant receptors for Wingless during Drosophila embryonic development. Development 126:4175–4186
16. Bhanot P, Brink M, Samos CH, Hsieh JC, Wang Y et al (1996) A new member of the frizzled family from Drosophila functions as a Wingless receptor. Nature 382:225–230
17. Pinson KI, Brennan J, Monkley S, Avery BJ, Skarnes WC (2000) An LDL-receptor-related protein mediates Wnt signalling in mice. Nature 407:535–538
18. Wehrli M, Dougan ST, Caldwell K, O'Keefe L, Schwartz S et al (2000) Arrow encodes an LDL-receptor-related protein essential for Wingless signalling. Nature 407:527–530
19. Tamai K, Semenov M, Kato Y, Spokony R, Liu C et al (2000) LDL-receptor-related proteins in Wnt signal transduction. Nature 407:530–535
20. Cselenyi CS, Jernigan KK, Tahinci E, Thorne CA, Lee LA et al (2008) LRP6 transduces a canonical Wnt signal independently of Axin degradation by inhibiting GSK3's phosphorylation of beta-catenin. Proc Natl Acad Sci U S A 105:8032–8037
21. Piao S, Lee SH, Kim H, Yum S, Stamos JL et al (2008) Direct inhibition of GSK3beta by the phosphorylated cytoplasmic domain of LRP6 in Wnt/beta-catenin signaling. PLoS One 3:e4046
22. Herz J, Strickland DK (2001) LRP: a multifunctional scavenger and signaling receptor. J Clin Invest 108:779–784
23. Qiu Z, Hyman BT, Rebeck GW (2004) Apolipoprotein E receptors mediate neurite outgrowth through activation of p44/42 mitogen-activated protein kinase in primary neurons. J Biol Chem 279:34948–34956
24. Shi Y, Mantuano E, Inoue G, Campana WM, Gonias SL (2009) Ligand binding to LRP1 transactivates Trk receptors by a Src family kinase-dependent pathway. Sci Signal 2:ra18
25. Krystosek A, Seeds NW (1981) Plasminogen activator release at the neuronal growth cone. Science 213:1532–1534
26. Krystosek A, Seeds NW (1984) Peripheral neurons and Schwann cells secrete plasminogen activator. J Cell Biol 98:773–776
27. Docagne F, Nicole O, Marti HH, MacKenzie ET, Buisson A et al (1999) Transforming growth factor-beta1 as a regulator of the serpins/t-PA axis in cerebral ischemia. FASEB J 13:1315–1324
28. Rogister B, Leprince P, Pettmann B, Labourdette G, Sensenbrenner M et al (1988) Brain basic fibroblast growth factor stimulates the release of plasminogen activators by newborn rat cultured astroglial cells. Neurosci Lett 91:321–326
29. Tsirka SE, Rogove AD, Bugge TH, Degen JL, Strickland S (1997) An extracellular proteolytic cascade promotes neuronal degeneration in the mouse hippocampus. J Neurosci 17:543–552
30. Kalderon N, Ahonen K, Fedoroff S (1990) Developmental transition in plasticity properties of differentiating astrocytes: age-related biochemical profile of plasminogen activators in astroglial cultures. Glia 3:413–426
31. Zheng S, Yin ZQ, Zeng YX (2008) Developmental profile of tissue plasminogen activator in postnatal Long Evans rat visual cortex. Mol Vis 14:975–982
32. Friedman GC, Seeds NW (1995) Tissue plasminogen activator mRNA expression in granule neurons coincides with their migration in the developing cerebellum. J Comp Neurol 360:658–670
33. Go HS, Shin CY, Lee SH, Jeon SJ, Kim KC et al (2009) Increased proliferation and gliogenesis of cultured rat neural progenitor cells by lipopolysaccharide-stimulated astrocytes. Neuroimmunomodulation 16:365–376
34. Slack RS, El-Bizri H, Wong J, Belliveau DJ, Miller FD (1998) A critical temporal requirement for the retinoblastoma protein family during neuronal determination. J Cell Biol 140:1497–1509

35. Shin CY, Choi JW, Jang ES, Ryu JH, Kim WK et al (2001) Glucocorticoids exacerbate peroxynitrite mediated potentiation of glucose deprivation-induced death of rat primary astrocytes. Brain Res 923:163–171
36. Lee WJ, Shin CY, Yoo BK, Ryu JR, Choi EY et al (2003) Induction of matrix metalloproteinase-9 (MMP-9) in lipopolysaccharide-stimulated primary astrocytes is mediated by extracellular signal-regulated protein kinase 1/2 (Erk1/2). Glia 41:15–24
37. Kim JW, Lee SH, Ko HM, Kwon KJ, Cho KS et al (2011) Biphasic regulation of tissue plasminogen activator activity in ischemic rat brain and in cultured neural cells: essential role of astrocyte-derived plasminogen activator inhibitor-1. Neurochem Int 58:423–433
38. Shin CY, Choi JW, Ryu JR, Ko KH, Choi JJ et al (2002) Glucose deprivation decreases nitric oxide production via NADPH depletion in immunostimulated rat primary astrocytes. Glia 37:268–274
39. Ding Y, Xi Y, Chen T, Wang JY, Tao DL et al (2008) Caprin-2 enhances canonical Wnt signaling through regulating LRP5/6 phosphorylation. J Cell Biol 182:865–872
40. Lee HY, Hwang IY, Im H, Koh JY, Kim YH (2007) Non-proteolytic neurotrophic effects of tissue plasminogen activator on cultured mouse cerebrocortical neurons. J Neurochem 101:1236–1247
41. Wei L, Cui L, Snider BJ, Rivkin M, Yu SS et al (2005) Transplantation of embryonic stem cells overexpressing Bcl-2 promotes functional recovery after transient cerebral ischemia. Neurobiol Dis 19:183–193
42. Salthouse TN (1964) Luxol fast blue G as a myelin stain. Stain Technol 39:123
43. Brennan K, Gonzalez-Sancho JM, Castelo-Soccio LA, Howe LR, Brown AM (2004) Truncated mutants of the putative Wnt receptor LRP6/Arrow can stabilize beta-catenin independently of Frizzled proteins. Oncogene 23:4873–4884
44. Tamai K, Zeng X, Liu C, Zhang X, Harada Y et al (2004) A mechanism for Wnt coreceptor activation. Mol Cell 13:149–156
45. Kundel M, Jones KJ, Shin CY, Wells DG (2009) Cytoplasmic polyadenylation element-binding protein regulates neurotrophin-3-dependent beta-catenin mRNA translation in developing hippocampal neurons. J Neurosci 29:13630–13639
46. Lucas FR, Salinas PC (1997) WNT-7a induces axonal remodeling and increases synapsin I levels in cerebellar neurons. Dev Biol 192:31–44
47. Lucas FR, Goold RG, Gordon-Weeks PR, Salinas PC (1998) Inhibition of GSK-3beta leading to the loss of phosphorylated MAP-1B is an early event in axonal remodelling induced by WNT-7a or lithium. J Cell Sci 111(Pt 10):1351–1361
48. Caricasole A, Ferraro T, Iacovelli L, Barletta E, Caruso A et al (2003) Functional characterization of WNT7A signaling in PC12 cells: interaction with A FZD5 x LRP6 receptor complex and modulation by Dickkopf proteins. J Biol Chem 278:37024–37031
49. Tzarfaty-Majar V, Lopez-Alemany R, Feinstein Y, Gombau L, Goldshmidt O et al (2001) Plasmin-mediated release of the guidance molecule F-spondin from the extracellular matrix. J Biol Chem 276:28233–28241
50. Park JE, Keller GA, Ferrara N (1993) The vascular endothelial growth factor (VEGF) isoforms: differential deposition into the subepithelial extracellular matrix and bioactivity of extracellular matrix-bound VEGF. Mol Biol Cell 4:1317–1326
51. Zhang L (2010) Glycosaminoglycan (GAG) biosynthesis and GAG-binding proteins. Prog Mol Biol Transl Sci 93:1–17
52. Zilberberg A, Yaniv A, Gazit A (2004) The low density lipoprotein receptor-1, LRP1, interacts with the human frizzled-1 (HFz1) and down-regulates the canonical Wnt signaling pathway. J Biol Chem 279:17535–17542
53. Kawata K, Kubota S, Eguchi T, Moritani NH, Shimo T et al (2010) Role of the low-density lipoprotein receptor-related protein-1 in regulation of chondrocyte differentiation. J Cell Physiol 222:138–148
54. Lindner I, Hemdan NY, Buchold M, Huse K, Bigl M et al (2010) Alpha2-macroglobulin inhibits the malignant properties of astrocytoma cells by impeding beta-catenin signaling. Cancer Res 70:277–287
55. Xia CH, Yablonka-Reuveni Z, Gong X (2010) LRP5 is required for vascular development in deeper layers of the retina. PLoS One 5:e11676
56. Castelo-Branco G, Andersson ER, Minina E, Sousa KM, Ribeiro D et al (2010) Delayed dopaminergic neuron differentiation in Lrp6 mutant mice. Dev Dyn 239:211–221
57. Parr BA, McMahon AP (1995) Dorsalizing signal Wnt-7a required for normal polarity of D-V and A-P axes of mouse limb. Nature 374:350–353
58. Yang Y, Niswander L (1995) Interaction between the signaling molecules WNT7a and SHH during vertebrate limb development: dorsal signals regulate anteroposterior patterning. Cell 80:939–947
59. Kim WY, Zhou FQ, Zhou J, Yokota Y, Wang YM et al (2006) Essential roles for GSK-3s and GSK-3-primed substrates in neurotrophin-induced and hippocampal axon growth. Neuron 52:981–996
60. Yu X, Malenka RC (2003) Beta-catenin is critical for dendritic morphogenesis. Nat Neurosci 6:1169–1177
61. Su F, Kozak KR, Herschman H, Reddy ST, Farias-Eisner R (2007) Characterization of the rat urokinase plasminogen activator receptor promoter in PC12 cells. J Neurosci Res 85:1952–1958
62. Hayden SM, Seeds NW (1996) Modulated expression of plasminogen activator system components in cultured cells from dissociated mouse dorsal root ganglia. J Neurosci 16:2307–2317
63. Asuthkar S, Gondi CS, Nalla AK, Velpula KK, Gorantla B et al (2012) Urokinase-type plasminogen activator receptor (uPAR)-mediated regulation of WNT/beta-catenin signaling is enhanced in irradiated medulloblastoma cells. J Biol Chem 287:20576–20589
64. Bukhari N, Torres L, Robinson JK, Tsirka SE (2011) Axonal regrowth after spinal cord injury via chondroitinase and the tissue plasminogen activator (tPA)/plasmin system. J Neurosci 31:14931–14943
65. Engelkamp D, Rashbass P, Seawright A, van Heyningen V (1999) Role of Pax6 in development of the cerebellar system. Development 126:3585–3596
66. Vaillant C, Meissirel C, Mutin M, Belin MF, Lund LR et al (2003) MMP-9 deficiency affects axonal outgrowth, migration, and apoptosis in the developing cerebellum. Mol Cell Neurosci 24:395–408
67. Gates MA, Tai CC, Macklis JD (2000) Neocortical neurons lacking the protein-tyrosine kinase B receptor display abnormal differentiation and process elongation in vitro and in vivo. Neuroscience 98:437–447
68. Malin D, Sonnenberg-Riethmacher E, Guseva D, Wagener R, Aszodi A et al (2009) The extracellular-matrix protein matrilin 2 participates in peripheral nerve regeneration. J Cell Sci 122:995–1004
69. Seeds NW, Basham ME, Haffke SP (1999) Neuronal migration is retarded in mice lacking the tissue plasminogen activator gene. Proc Natl Acad Sci U S A 96:14118–14123
70. Xin H, Li Y, Shen LH, Liu X, Wang X et al (2010) Increasing tPA activity in astrocytes induced by multipotent mesenchymal stromal cells facilitate neurite outgrowth after stroke in the mouse. PLoS One 5:e9027
71. Lin YC, Ko TL, Shih YH, Lin MY, Fu TW et al (2011) Human umbilical mesenchymal stem cells promote recovery after ischemic stroke. Stroke 42:2045–2053
72. Shen LH, Li Y, Chopp M (2010) Astrocytic endogenous glial cell derived neurotrophic factor production is enhanced by bone marrow stromal cell transplantation in the ischemic boundary zone after stroke in adult rats. Glia 58:1074–1081
73. Bao X, Wei J, Feng M, Lu S, Li G et al (2011) Transplantation of human bone marrow-derived mesenchymal stem cells promotes behavioral recovery and endogenous neurogenesis after cerebral ischemia in rats. Brain Res 1367:103–113